Abstract

Haptic Teleoperation of a Pair of WMRs with Mixed Physical/Virtual Constraints

Hyunjun Cho
Mechanical & Aerospace Engineering
The Graduate School
Seoul National University

A novel framework of haptic teleoperation of a pair of nonholonomic wheeled mobile robots with mixed physical/virtual constraints is presented in this thesis. The proposed framework enables a remote single user to teleoperate the overall motion, while cooperatively squeeze-grasping a common deformable object. Under the mixed constraint, although master interface is free to move, the slave robots have limitation about their motion. To accept/accommodate the mixed constraint, we design haptic feedback and local autonomous control following human command with feasible set, which is defined by all possible motion under mixed constraint on the instant. For mathematical expression, nonholonomic passive decomposition [1, 2] is utilized to decompose the overall motion into the two aspects: grasping shape system and locked overall system. Using theses two aspects, we design semi-autonomous teleoperation architecture where a haptic feedback is designed to inform the human user of feasible command direction, while a local autonomous control drives the pair to follow the human command as much as permissible by the mixed constraint. Real experiment is also performed to support the theory.

Keywords: Asymmetric teleoperation, Mixed constraint, Wheeled mobile robot, Haptic feedback, Semi-autonomous, Feasibility

Student Number: *2012-23193*

Contents

List of Figures

Abbreviations

WMR	**W**heeled **M**obile **R**obot
NPD	**N**onholonomic **P**assive **D**ecomposition
DOF	**D**egree **O**f **F**reedom
IC	**I**nstantaneous **C**enter
FPV	**F**ront **P**oint **V**iew
IMU	**I**nertial **M**easurement **U**nit

Symbols

$\{\mathcal{I}\}$	Inertial frame
$\{\mathcal{B}\}$	Body-fixed frame
$\{\mathcal{H}\}$	Haptic frame

Chapter 1

Introduction

1.1 Motivation and Objectives

Let us consider a pair of WMRs maneuvering together while maintaining their distance and squeezing/grasping a common deformable object. Then, from their behavior, we can think the two fundamental aspects: 1) grasping shaping aspect describing the pair's shape; 2) maneuvering aspect representing the pair's overall motion. These decoupling of group behavior is desirable because that means that it's possible to control these two aspects individually and separately. For example, imagine a scenario where, without such decoupling, the pair maneuver together while grasping shape. Due to grasp-maneuver coupling, whenever the

pair often change their velocity, the grasping shape will be perturbed by maneuvering dynamics, while the pair will drop the grasped object. Therefore, when we utilize the pair in real applications like house, factory, and unstructured outdoor, these grasp-maneuver decoupling and individually/separately controlling ability are imperative.

Meanwhile, utilizing the pair in applications mentioned above, it is natural for human command to be included because environment where the pair are employed would be complex and unpredictable in many cases. Thus, teleoperation is highly favored in dealing with such dynamic environment. However, when teleoperating the pair, we confront an issue of mixed constraint. Nonholonomically constrained WMR inherently has 2-DOFs, i.e., forward/angular direction, but each WMR of the pair has 1-DOF because the pair's inherent motion is limited by virtual constraint oriented from the grasping shape task. Therefore, under the mixed constraint, it is challenging for human user to teleoperate the pair while cooperatively squeezing/grasping a common object due to their insufficient DOF. To accept/accommodate the mixed constraint when teleopeating the pair, we define feasible set as all possible motion of robots under the mixed constraint on the instant. Considering the feasible set, we design haptic feedback and local autonomous control following human command, which are designed to inform the human user of feasible command direction and draw the pair toward human command as much as permissible by the mixed constraint respectively.

From the above motivations, in this thesis, the objective of our research is to

provide a haptic teleoperation framework of a pair of WMRs with mixed constraint. To accept/accommodate the mixed constraint, we also provide the design of haptic feedback and local autonomous control. Ultimately, we are interested in realization of our framework in outdoor environment with FPV camera and its extension. For this, we start from the case where a pair of kinematic WMRs cooperatively grasp/transport a common object in indoor environment with motion-capture system.

1.2 Challenges

There are two main challenges originated from the pair's constrained motion when we establish our objective.

First challenge lies in the mixed constraint, which arises from simultaneous effect of physically nonholonomic constraint and virtual grasping constraint. This challenge has relation to the question of how can we enforce virtual grasping constraint under nonholonomic constraint. Thus, we should consider virtual grasping constraint under nonholonomic constraint. Here, we utilize a previously-proposed NPD. [1, 2] The added terminology 'passive'means that this theory fundamentally realizes decomposition of dynamic system, however, by exploiting decomposition of velocity space instead of force space, it can be clearly used in kinematic system. By using NPD, we can completely decompose unconstrained system into the two aspects: 1) grasping shape system describes the cooperative grasping

shape; 2) locked system describes the pair's overall motion. From these two decoupling, we can control these two systems individually/separately: 1) local autonomous grasping shaped control to achieve precise grasping; 2) locked system control to carry a grasped object. In other words, using NPD, we can decompose the mixed constrained system into the two aspects and control these aspects individually/separately.

The second challenge lies in constrained teleoperation. This challenge is about the question of how to teleoperate the pair of WMRs under overly constrained system. Overly constrained condition means that slave-DOF is limited compared to master-DOF due to the mixed constraint. Under overly constrained system, although master interface is free to move, the WMRs have limitation about their motion. As a result, Overly constrained system doesn't have symmetric teleoperation property because of insufficient slave-DOFs. Overly constrained system has an innate asymmetric property, which is a terminology previously referred to [3]. To teleoperate overly constrained system or accept/accommodate the mixed constraint when teleoperating the pair, here, we propose not only semi-autonomous control architecture with autonomous control following human command but also haptic feedback design reporting feasible command direction. For this, with suitable haptic interface, we define feasible set, which is all possible motion under the mixed constraint on the instant, exploited to design the haptic feedback and the local autonomous control.

1.3 Relevant Work and Contribution

Many researches using various mobile platform, e.g., multiple WMRs [4–8], single WMR [9–11], mobile manipulator [12–15], and so on, already have been presented. Further, a number of researches based on passive decomposition have been presented about muiti-mobile robot. (e.g., [1, 14, 16, 17]).

Apart from these results, researches relevant to the haptic teleoperation have been studied so far. Focusing on DOF of master and slave, the majority of teleoperation results consider only symmetric teleoperation. [18–21] Symmetric teleoperation means that master-DOF is same with slave-DOF. Therefore, they mainly deal with single agent as slave. On the other hand, there are a lot of results on multiple WMR/UAV as slave. Here, teleoperation of multiple WMR/UAV typically considers redundant slave, not overly constrained slave system. [22–26] It is conceptually clear to us that redundant slave system would be realizable due to its high slave-DOF ensuring high capability for control.

To our knowledge, there are only few recent results on similar problem with our study. [3] The research is about teleoperation of manipulator that is remotely teleoperated by multi-users. Because of increased master-DOF, the overall system can be referred as an asymmetric teleoperation system. In contrast to our case, system constraint is imposed not by task but by only system itself. In other words, the constraint in the research is all physical and master-DOF is artificially increased to resolve it. The solution is also different from our study. Our solution

based on teleoperation by a single user is to design haptic feedback and autonomous control following human command, whereas they first put multi-users for teleoperation and then teleoperate separately by their decomposition.

Unlike these results for haptic teleoperation and coordination control, in this research, our haptic teleoperation framework proposes: 1) NPD-based virtual grasp constraint control under no-slip constraint while rigidly rotating formation; 2) a novel semi-autonomous control architecture for overly constrained teleoperation; 3) experimental implementation and verification.

The rest of this thesis is organized as follows. Sec. 2 contains some preliminary background materials on system. In Sec. 3, we divide the system into two fundamental aspects by using NPD and Sec. 4 presents how to design haptic feedback and autonomous human command control considering feasibility. Setup and results of real experiment are presented in Sec. 5. Finally, concluding remarks is in Sec. 6.

Chapter 2

System Description

2.1 System Model

We consider two WMRs like Fig. 2.1. This is starter case transporting a grasped common object although other construction can be applied. i-th WMR's configuration that specifies WMR's position is given by configuration $q_i = [x_i \ y_i \ \phi_i]^T \in \Re^3$, where i=$\{1, 2\}$ is numbering index of WMR, $(x_i \ y_i)$ is position of geometric center of i-th WMR measured in the $\{\mathcal{I}\}$, ϕ_i is heading angle of i-th WMR from x-axis of $\{\mathcal{I}\}$ or, equivalently, angle between $\{\mathcal{I}\}$ and $\{\mathcal{B}\}$.

The i-th WMR has following nonholonomic Pfaffian constaint [27]:

$$A_i(q_i)\dot{q}_i = 0 \tag{2.1}$$

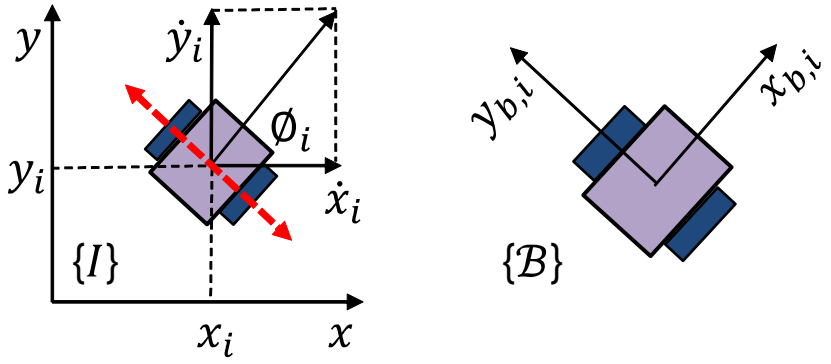

FIGURE 2.1: Geometry of WMR w.r.t $\{\mathcal{I}\}$ and $\{\mathcal{B}\}$, the dotted bilateral arrow which indicates nonholonomic constraint.

with $A_i(q_i) \in \Re^{1\times 3}$ is

$$A_i(q_i) := \begin{bmatrix} \sin(\phi_i) & -\cos(\phi_i) & 0 \end{bmatrix} \tag{2.2}$$

Widely known Pfaffian constraint $A_i(q_i)$ represents no side-way slip condition or nonholonomic constraint of i-th WMR. (2.1) and (2.2) are encoded by integrated Pfaffian constraint as follows:

$$A(q)\dot{q} = 0 \tag{2.3}$$

where $q := [q_1; q_2]$ and $A(q)$:= diag$[A_1(q_1)\ A_2(q_2)] \in \Re^{2\times 6}$. Respecting this integrated constraint, the overall WMRs' motion $\dot{q}$ is restricted in null-space of $A(q)$,

i.e.,

$$\dot{q} \in \text{null}(A(q)) =: D_{\top}(q) \tag{2.4}$$

where

$$D_{\top}(q) = span \begin{bmatrix} \cos(\phi_1) & 0 & 0 & 0 \\ \sin(\phi_1) & 0 & 0 & 0 \\ 0 & 1 & 0 & 0 \\ 0 & 0 & \cos(\phi_2) & 0 \\ 0 & 0 & \sin(\phi_2) & 0 \\ 0 & 0 & 0 & 1 \end{bmatrix} \tag{2.5}$$

where $D_{\top}(q)$, with $\dim(D_{\top}(q))$=4, is *unconstrained distribution* [27] of the (2.3). $D_{\top}$ indicates direction of unconstrained motion respecting nonholonomic constraint. That is, (2.4) means that $\dot{q}$ should be in $D_{\top}$ to freely move in unconstrained direction while respecting nonholonomic constraint (2.3). Meanwhile, equivalently, the motion of WMRs $\dot{q}$ is evolved as

$$\dot{q} = D_{\top} \begin{pmatrix} v_1 \\ \omega_1 \\ v_2 \\ \omega_2 \end{pmatrix} \tag{2.6}$$

where v_i, ω_i, $\dot{q}$ are body-fixed forward, angular velocity of i-th WMR, and velocity in $\{\mathcal{I}\}$ respectively. From (2.6), we take $[v_1;\omega_1;v_2;\omega_2]$ as control input u dominating motion of overall kinematic system.

2.2 Grasping Shape Map

Let us consider grasping constraint not losing generality. To transport an object cooperatively, we assume that WMRs grasp a common deformable object under the following condition:

$$q_E(q(t)) \to q_E^d \tag{2.7}$$

where q_E is grasping shape map. Also, q_E^d is a constant vector specifying desired grasping shape. q_E is smooth function and we call q_E *grasping shape function*. Under the condition (2.7), WMRs transport a grasped object with *fixture-less grasping*, which means that WMRs cooperatively grasp a common object while squeezing it to achieve (2.7) with no contact-enforcing fixture. Note that q_E can be changed by task or user-specific shape. See. Fig. 2.2. We define the grasping shape function s.t.

$$q_E = \begin{bmatrix} x_1 - x_2 - L\cos(\phi_2) \\ y_1 - y_2 - L\sin(\phi_2) \end{bmatrix} \tag{2.8}$$

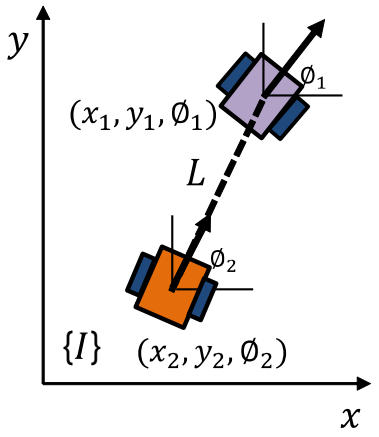

FIGURE 2.2: Graphical description of grasping shape function, i.e., if $q_E^d = 0$, then $x_1 = x_2 + \cos(\phi_2)$ and $y_1 = y_2 + \sin(\phi_2)$.

where L is distance between geometric center of the first/second WMR. The grasping shape function (2.8) is similar with that of [17]. If desired grasping shape q_E^d=0, the two WMRs will form a rigid rod whose length is L. Note that rotation of the rod is specified by the second WMR's yaw angle whose teleoperation would ensure flexibility and ease of navigation in real application like house, factory and so on. Here, total-DOF is 4 in $D_\top$, yet, constrained-DOF by condition q_E^d=0 is 2, thus negotiated motion of WMRs is in the remaining 2-DOF. We should use the remaining 2-DOF for teleoperation except the overlapped 2-DOF.

To describe motion of WMRs respecting or not respecting virtual grasping constraint, we express q_E by Lie derivative [27, 28] along $\dot{q}$ from (2.7)

$$\mathcal{L}_{\dot{q}} q_E = \frac{\partial q_E}{\partial q} \dot{q} = 0 \tag{2.9}$$

$$\frac{\partial q_E}{\partial q}\dot{q} = \begin{bmatrix} 1 & 0 & 0 & -1 & 0 & L\sin(\phi_2) \\ 0 & 1 & 0 & 0 & -1 & -L\cos(\phi_2) \end{bmatrix} \dot{q} = 0$$

$\mathcal{L}_{\dot{q}} q_E$ is Lie derivative of q_E along $\dot{q}$. The equation (2.9) defines virtual grasping constraint. Meanwhile, by the definition from [1, 2], we get following two distributions for virtual grasping constraint:

$$\triangle_\top := \text{null}(\partial q_E / \partial q) \tag{2.10}$$

$$\triangle_\perp := \text{row}(\partial q_E / \partial q) \tag{2.11}$$

where 1) $\triangle_\top$ is *parallel distribution* not affecting grasping shape; 2) $\triangle_\perp$ is *normal distribution* affecting grasping shape. [1, 2] $\triangle_\top$ is direction of motion respecting virtual grasping constraint, i.e., motion direction not perturbing grasping shape and $\triangle_\perp$ is direction of motion not respecting virtual grasping constraint, i.e., motion direction changing grasping shape. For reference, you can find details in [1, 2].

Chapter 3

Nonholonomic Passive Decomposition

3.1 Nonholonomic Passive Decomposition

One of the important challenges is that motion of the two WMRs is under mixed constraint, i.e., overly constrained system. Let's see Fig. 3.1 describing this graphically. The figure shows that teleoperation of overly constrained WMRs is under lack of DOF.

Because of IC, the second WMR has 1-DOF motion about IC. Additionally, because the first WMR has 1-DOF motion for its rotation, the two WMRs have 2-DOF motion totally. On the other hand, for teleoperation, master has 1-DOF

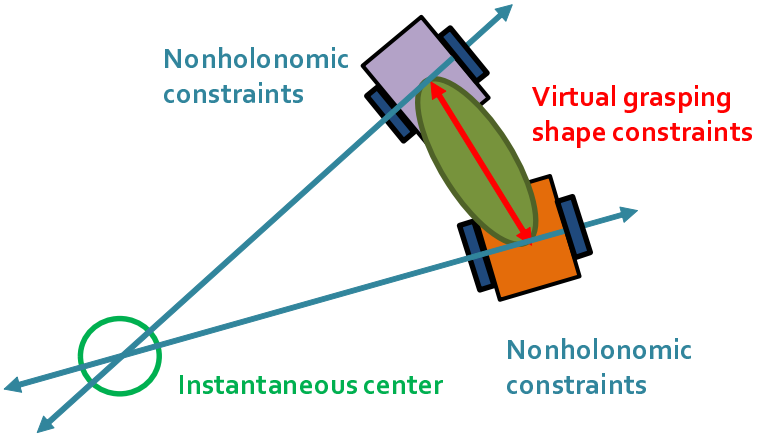

FIGURE 3.1: Graphical representation of mixed constraint;
slave DOF = 1-DOF WMR2 motion about IC + 1-DOF WMR1 rotation;
master DOF = 1-DOF for WMR2 forward + 1-DOF WMR2 angular velocity.

for forward driving and 1-DOF for angular steering. As a result, we can not tele-drive each WMR completely due to their insufficient DOF.

To solve an insufficient DOF problem of each WMR while teleoperating, given mathematically represented physical no-slip constraint (2.3), virtual grasping constraint (2.9), and kinematics (2.6), by using NPD [1, 2], we decompose *unconstrained distribution* (2.5) into the following:

$$D_{\top} = (D_{\top} \cap \triangle_{\top}) \oplus (D_{\top} \cap \triangle_{\perp}) \tag{3.1}$$

With (3.1), we express (2.6) as follows:

$$\dot{q} = [D_\top \cap \triangle_\top \;\; D_\top \cap \triangle_\perp] \begin{pmatrix} u_L \\ u_E \end{pmatrix} \tag{3.2}$$

where $[D_\top \cap \triangle_\top \;\; D_\top \cap \triangle_\perp] =: S(q)$ is decomposition matrix. $u_L \in \Re^2$, $u_E \in \Re^2$ are locked system and grasping shape system control input respectively. Because the motion of two WMRs is split into these two systems precisely, we can simply control these separately.

Meanwhile, since the above decomposed input, i.e.,$[u_L; u_E]$, is not an actual input for system (2.6), we have to decode (3.2) with (2.6) to obtain an actual input u in practice s.t.

$$u = (D_\top^T D_\top)^{-1} D_\top^T S(q) \begin{pmatrix} u_L \\ u_E \end{pmatrix} \tag{3.3}$$

where $u = [v_1; \omega_1; v_2; \omega_2]$. Detailed design for u_E and u_L is in Sec. 3.2 and 4.3 respectively. In following sections, we look for locked distribution ($D_\top \cap \triangle_\top$) and grasping shape distribution ($D_\top \cap \triangle_\perp$).

3.1.1 Locked Distribution

We obtain locked distribution by same procedure [1, 2] s.t.

$$[D_\top \cap \triangle_\top] = span \begin{bmatrix} Lc\phi_1 & 0 \\ Ls\phi_1 & 0 \\ 0 & 1 \\ Lc(\phi_1 - \phi_2)c\phi_2 & 0 \\ Lc(\phi_1 - \phi_2)s\phi_2 & 0 \\ s(\phi_1 - \phi_2) & 0 \end{bmatrix} \tag{3.4}$$

where $\mathrm{c}\phi_i = \cos\phi_i$, $\mathrm{s}\phi_i = \sin\phi_i$, $i = \{1, 2\}$. With the equation (3.4), we define motion not perturbing grasping shape while respecting physical nonholonomic constraint. Considering $\dot{q}_L = [D_\top \cap \triangle_\top]u_L$, which $u_L \in \Re^2$ constitutes forward and angular velocity command, the equation (3.4) then constructs motion of direction of locked system. The First column of (3.4) represents forward-coordinated motion of WMRs while the second represents their rotation. Using the second column, we can control the rotation of first WMR, not that of second WMR. That means that the first WMR has DOF for rotation while the second WMR doesn't. Note that if we deal with problem of simple fixed-vectorial formation, we can readily control the second WMR's rotation, however, in (3.4), we can't control the second WMR's rotation because the last entry of second column is zero, not equal to one. Here, using the last entry of first column, we can control

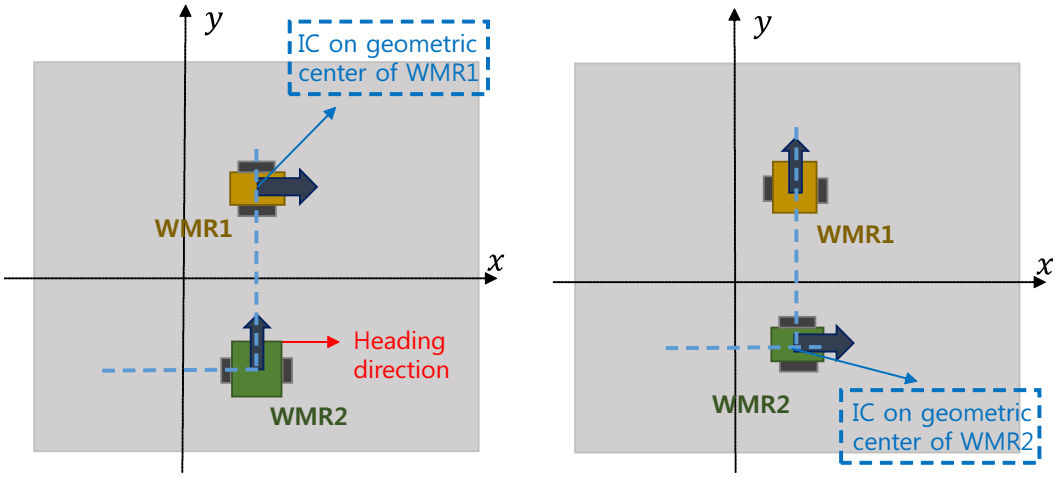

FIGURE 3.2: Singularities caused by position of IC

the second WMR's rotation. For this, we adequately establish haptic interface in Sec. 4.1.

Meanwhile, let us consider certain geometrical configuration (i.e., $\phi_1 - \phi_2 = n\pi + \frac{\pi}{2}$, $n = \{0, 1, 2 \cdots\}$) in Fig. 3.2. In these configuration, the forward velocity of 2^{nd} WMR stays zero. ($\because \cos(\phi_1 - \phi_2) = 0$) This observation corresponds with the situation, where the IC of two WMRs is exactly located in geometric center of one WMR. As Fig. 3.2, the WMRs then can not move straight on the instant.

Here, we define singularity as the situation that the two WMRs can't go straight but rotate only. To avoid singularity, ϕ_1, ϕ_2 should be in the certain region of motion, which is graphically described in Fig. 3.3. If ϕ_1, ϕ_2 stay in the region in Fig. 3.3, singularity doesn't occur, In Sec. 4, including teleoperation, with suitable teleoperation interface, we will deal with feasibility of motion.

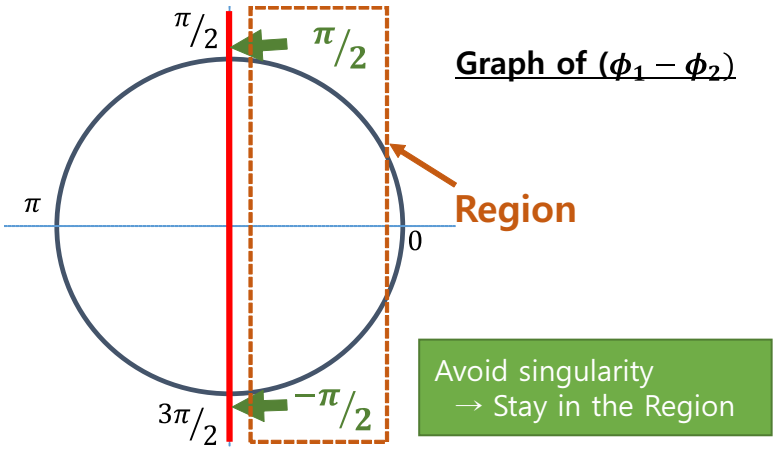

FIGURE 3.3: $(\phi_1 - \phi_2)$ graph and region of non-singularity

3.1.2 Grasping Shape Distribution

By same calculation with Sec. 3.1.1, we can compute grasping shape distribution s.t.

$$[D_\top \cap \triangle_\perp] = span \begin{bmatrix} -c\phi_2 & 1 \\ -s\phi_2 & 0 \\ 0 & 0 \\ c\phi_2 & -1 \\ s\phi_2 & 0 \\ 0 & Ls\phi_2 \end{bmatrix} \tag{3.5}$$

The equation (3.5) describes direction changing virtual grasping shape while still respecting nonholonomic constraint, and it directly changes grasping shape with

$u_E \in \Re^2$. i.e., $\dot{q}_E = [D_\top \cap \triangle_\perp] u_E$. With (3.5), we activate an autonomous grasping shape control to adjust shape while user takes care of tele-drive completely. In other words, we regulate shape system by autonomous shape control and teleoperate locked system. Essentially, we should inspect whether the above two columns are contained in $\triangle_\top$ or not. If the bases of (3.5) only belongs to $\triangle_\perp$, any column vector of (3.5) would be orthogonal to (3.4), otherwise, the above bases would be in $\triangle_\top$ too. Note that the bases of some grasping shape distribution can be in both $\triangle_\top$ and $\triangle_\perp$, i.e., strong/weak decomposibility [1].

3.2 Grasping Shape Control

Following [1, 2], we can design grasping shape system control u_E s.t.

$$u_E = -S_E(q) \left[\frac{\partial \varphi_E}{\partial q_E} \right]^T \tag{3.6}$$

$$S_E := (D_\top \cap \triangle_\perp)^T \left[\frac{\partial q_E}{\partial q} \right]^T \tag{3.7}$$

where φ_E is potentials, e.g., $\varphi_E(q_E) = \frac{1}{2}(q_E - q_E^d)^T k_E (q_E - q_E^d)$, and its partial derivatives w.r.t. q_E plays a role such as P control. S_E only decides direction of control by removing direction from nonholonomic constraint. With u_E, we can send q_E to q_E^d. Meanwhile, the result in [1], $\varphi_E(q_E(t)) \leq \varphi_E(q_E(0))$, implies that the control enforces $q_E(t) = q_E(0)$ if WMRs start with desired shape. That means that the two WMRs successfully transport a grasped object while squeezing it for all $t \geq 0$.

With (3.2),(3.4) and (3.5), we combine these representation as follows:

$$\dot{q} = \dot{q}_L + \dot{q}_E = \begin{bmatrix} Lc\phi_1 & 0 \\ Ls\phi_1 & 0 \\ 0 & 1 \\ Lc(\phi_1 - \phi_2)c\phi_2 & 0 \\ Lc(\phi_1 - \phi_2)s\phi_2 & 0 \\ s(\phi_1 - \phi_2) & 0 \end{bmatrix} u_L + \begin{bmatrix} -c\phi_2 & 1 \\ -s\phi_2 & 0 \\ 0 & 0 \\ c\phi_2 & -1 \\ s\phi_2 & 0 \\ 0 & Ls\phi_2 \end{bmatrix} u_E$$

Like above, we split WMRs' motion into locked system and shape system. We thus can control these systems separately. Using (3.6), we regulate grasping shape autonomously and teleoperate locked system. The design of u_L is in Sec. 4.3.

Chapter 4

Haptic Teleoperation

4.1 Haptic Interface

First, our haptic device is coordinated as Fig. 4.1. The figure simply shows a coordination of master frame, which can be replaced with other coordination alternatively. With this coordination, to tele-drive the two WMRs intuitively for human user, we design haptic interface s.t.

$$\begin{pmatrix} v_h \\ \omega_h \end{pmatrix} = \begin{pmatrix} \eta_1 q_y(t) \\ \eta_2 \tan^{-1}(q_x(t)/q_y(t)) \end{pmatrix} \tag{4.1}$$

where v_h, ω_h is forward and angular velocity command from teleoperation respectively. $q_{x,y}(t) \in \Re$ is X,Y position of haptic device in $\{\mathcal{H}\}$ and $\eta_{1,2}$ acts as

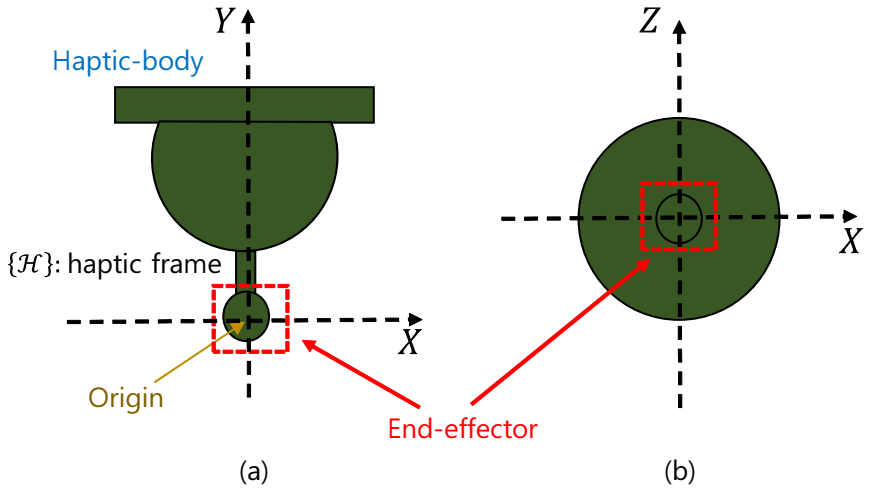

FIGURE 4.1: Coordination of master frame $\{\mathcal{H}\}$. (a): view of haptic device from above, (b): view of haptic device from front.

teleoperation gain, which is matching constant between teleoperation velocity command and haptic position. Generally, slave workspace is unlimited and, on the other hand, master workspace is usually limited. Considering this difference between the workspace of slave and master, using $\eta_{1,2}$, we can successfully resolve the problem of dissimilarity. In other words, we utilize the position of master to make the teleoperation velocity command using the matching constant $\eta_{1,2}$. Meanwhile, the $\tan^{-1}$ function is included in ω_h for smooth steering. When human user begins to turn a head of maneuvering of the WMRs, we should consider aggressive motion of them. If other modality of steering is utilized, (e.g., $q_x(t)$) it should cover aggressive motion of maneuvering, otherwise, the shape or maneuvering may be deviated from desired one because of their physical limitation.

Note that the haptic interface (4.1) is one example and other interface would be able to replace it.

Here, we construct the important aspect of haptic interface by relating teleoperation velocity command (v_h, ω_h) to locked system control u_L in (3.2) s.t.

$$\begin{pmatrix} v_h = Lc(\phi_1 - \phi_2)u \\ \omega_h = s(\phi_1 - \phi_2)u \end{pmatrix} \tag{4.2}$$

where u and $\dot{\phi}_1 \in \Re$ are forward and rotation command of u_L respectively. (i.e., $[u; \dot{\phi}_1] = u_L$) The teleoperation velocity command (v_h,ω_h) is made by (4.1). Combining (4.1) with (4.2), we relate position of haptic device with locked system control, i.e.,

$$\begin{pmatrix} \eta_1 q_y(t) \\ \eta_2 \tan^{-1}(q_x(t)/q_y(t)) \end{pmatrix} = \begin{pmatrix} Lc(\phi_1 - \phi_2)u \\ s(\phi_1 - \phi_2)u \end{pmatrix}$$

Meanwhile, importantly, the equation (4.2) means that human user controls the second WMR directly. We can check it in follows:

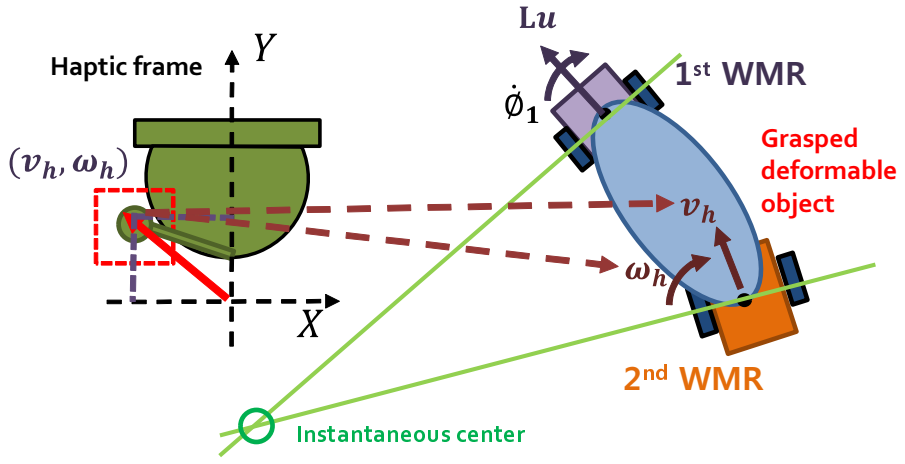

FIGURE 4.2: To complement insufficient slave-DOF, human teleoperates WMR2 directly and WMR1 indirectly; (v_h, ω_h)→WMR2 and $(u, \dot{\phi}_1)$→WMR1.

$$\dot{q}_L = [D_\top \cap \triangle_\top] u_L = \begin{bmatrix} Lc\phi_1 & 0 \\ Ls\phi_1 & 0 \\ 0 & 1 \\ Lc(\phi_1 - \phi_2)c\phi_2 & 0 \\ Lc(\phi_1 - \phi_2)s\phi_2 & 0 \\ s(\phi_1 - \phi_2) & 0 \end{bmatrix} \begin{pmatrix} u \\ \dot{\phi}_1 \end{pmatrix} \tag{4.3}$$

Note that $[u; \dot{\phi}_1] = u_L \in \Re^2$. We can see that the fourth-sixth entries constitute the second WMR's velocities. The fourth and fifth entries have $\cos\phi_2$ and $\sin\phi_2$ respectively. Therefore, together with $L\cos(\phi_1 - \phi_2)$, we exactly create the x, y velocity of second WMR from v_h. Additionally, ω_h corresponds to the rotation

velocity of second WMR. i.e.,

$$\dot{q}_{2,L} = \begin{pmatrix} \dot{x}_{2,L} \\ \dot{y}_{2,L} \\ \dot{\phi}_{2,L} \end{pmatrix} = \begin{pmatrix} v_h c\phi_2 \\ v_h s\phi_2 \\ \omega_h \end{pmatrix}$$

where $\dot{q}_{2,L} \in \Re^3$ is the velocity of second WMR. Similarly, $\{\dot{x}, \dot{y}, \dot{\phi}\}_{2,L} \in \Re$ are x,y velocity, and angular velocity of the second WMR respectively. Note that $v_h = Lu\cos(\phi_1 - \phi_2)$ and $\omega_h = u\sin(\phi_1 - \phi_2)$ from the haptic interface equation (4.2). From above equation, we can see that the second WMR's forward/angular velocity are generated from teleoperation velocity command (v_h, ω_h) directly, i.e., human user tele-drive the second WMR directly. Then, in reverse, using u,$\dot{\phi}_1$, we generate the first WMR's velocity. i.e.,

$$\dot{q}_{1,L} = \begin{pmatrix} \dot{x}_{1,L} \\ \dot{y}_{1,L} \\ \dot{\phi}_{1,L} \end{pmatrix} = \begin{pmatrix} uLc\phi_1 \\ uLs\phi_1 \\ \dot{\phi}_1 \end{pmatrix}$$

where $\{\dot{q}, \dot{x}, \dot{y}, \dot{\phi}\}_{1,L}$ have same definitions with $\{\dot{q}, \dot{x}, \dot{y}, \dot{\phi}\}_{2,L}$ but w.r.t. first WMR. We can say that this reversed process for the first WMR is indirect process w.r.t. teleoperation velocity command because we are using $\{u, \dot{\phi}_1\}$ here. not (v_h, ω_h). (See. Fig. 4.2). Note that uL, $\dot{\phi}_1$ is forward/angular velocity of first WMR.

4.2 Feasible Set

As mentioned in Sec. 3, there exist feasible motion for the two WMRs at any instant. Here, we define $feasible\ set$ as collection of feasible motion of slave via master frame. Systematically, if slave has no constraint, feasible set is master workspace itself. Thus, when slave has an any constraint, feasible set appears in the form of limited. Here, we establish feasible set in $\{\mathcal{H}\}$.

Recall the haptic interface (4.1). we rearrange our haptic interface. as follows:

$$u = \frac{v_h}{L\cos(\phi_1 - \phi_2)} = \frac{\omega_h}{\sin(\phi_1 - \phi_2)}$$

Then, we assign v_h to Y and ω_h to X where X,Y is x,y coordination in $\{\mathcal{H}\}$, i.e., coordination of haptic frame. Considering (4.1), (i.e., $\eta_1 q_y(t) = v_h$ and $\eta_2 \tan^{-1}(q_x(t)/q_y(t)) = \omega_h$) assignment ω_h to X may be inexact somewhat but there is no big failure because, with multiplying with η_2, $\tan^{-1}(q_x(t)/q_y(t))$ can be approximated by $q_x(t)$. Using haptic coordination X,Y, we can rewrite the above expression into haptic frame.

$$\frac{\mathrm{Y}}{L\cos(\phi_1 - \phi_2)} = \frac{\mathrm{X}}{\sin(\phi_1 - \phi_2)}$$

This leads to new expression s.t.

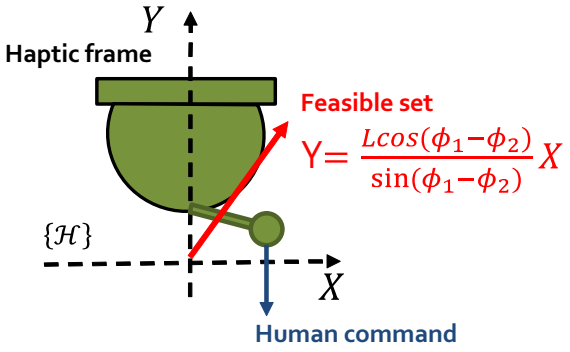

FIGURE 4.3: Feasible set and human command in $\{\mathcal{H}\}$

$$\mathrm{Y} = \frac{L\cos(\phi_1 - \phi_2)}{\sin(\phi_1 - \phi_2)}\mathrm{X} \tag{4.4}$$

This is feasible set about mixed constraint. (See. Fig. 4.3) Note that the feasible set reflects the current state of WMRs (i.e., ϕ_1,ϕ_2) since the feasible motion of the WMRs would be varying with their angular position.

Meanwhile, feasible set is thought of as system interpretation about feasible motion of slave. Feasible set as system interpretation helps to establish not only the criterion for design of local control to follow human command but also the criterion for design of haptic feedback. The following Sec. 4.3, 4.4 deal with local autonomous control to follow human command and haptic feedback respectively.

4.3 Locked Control to follow Human Command

We want teleoperate forward/angular velocities of second WMR. However, as confirmed in equation (4.3), the genearation of rotating motion of second WMR is only possible through u in u_L. (i.e., $\dot{\phi}_{2,L} = u\sin(\phi_1 - \phi_2)$) Meanwhile, with the second column in (4.3), we can freely control ϕ_1 and this controlled ϕ_1 changes ϕ_2 about IC because $\dot{\phi}_{2,L} = u\sin(\phi_1 - \phi_2)$. Therefore, here, we compute the desired set value (u, ϕ_1^d) according to teleoperation velocity command (v_h, ω_h) and then design control input $\dot{\phi}_1$ tracking ϕ_1^d (i.e., $\phi_1 \to \phi_1^d$), which changes ϕ_2 about IC.

Assume that $\phi_1 \to \phi_1^d$. Then, we put up the two equations from (4.2) s.t.

$$\begin{pmatrix} v_h = L\cos(\phi_1^d - \phi_2)u \\ \omega_h = \sin(\phi_1^d - \phi_2)u \end{pmatrix} \tag{4.5}$$

where v_h, ω_h, ϕ_2 are all known because v_h, ω_h are teleoperation command inputs and ϕ_2 is state measured from some sensor while u, ϕ_1^d are unknown that we are looking for. With the equation (4.5), we easily obtain u, ϕ_1^d because there are two unknowns and two equations. i.e.,

$$\phi_1^d = \phi_1^d(v_L, \omega_L, \phi_2)$$
$$u = u(v_L, \omega_L, \phi_2)$$

Here, we solve the equation (4.5). u, ϕ_1^d are as follows:

$$\phi_1^d = \phi_2 + \tan^{-1}(\frac{L\omega_h}{v_h}) \tag{4.6}$$

$$u = \frac{v_h}{L}\sec(\tan^{-1}(\frac{L\omega_h}{v_h})) \tag{4.7}$$

Here, we obtain physical insight of *Case* (1-4) from (4.6),(4.7).

Case 1. ($\omega_h \neq 0$, $v_h \neq 0$) :
Case 1 is general case. As Fig. 4.4(a), motion about IC can be uniquely found. When $\omega_h \neq 0$, $v_h \neq 0$, ϕ_1^d is determined by position ϕ_2 uniquely. In other words, the desired position of first WMR is unique when the second WMR's position is determined. With unique ϕ_1^d, u is also uniquely determined in this configuration. ($\because u = \omega_h / \sin(\phi_1^d - \phi_2)$).

Case 2. ($\omega_h = 0$, $v_h \neq 0$) :
In *case* 2, we get the result that $\tan^{-1}(\frac{L\omega_h}{v_h}) = n\pi$ and $\phi_1^d = \phi_2 + n\pi$. ($n = 0, 1, 2\cdot\cdot$) That means that the feasible motion of two WMRs is going straight and it makes sense to the condition of *case* 2, i.e., $\omega_h = 0$, $v_h \neq 0$. In Fig. 4.4(b), we can see this physically.

Case 3. ($\omega_h \neq 0$, $v_h = 0$) :
In *case* 3, we get the result that $\tan^{-1}(\frac{L\omega_h}{v_h}) \rightarrow (n\pi + \frac{\pi}{2})$ and $\phi_1^d = \phi_2 + (n\pi + \frac{\pi}{2})$. ($n = 0, 1, 2\cdot\cdot$) The Fig. 4.4(c),(d) show this situation physically. The configuration in the Fig. 4.4(c),(d) corresponds to singularity because orthogonal vector to one WMR's velocity passes through the other WMR's geometric center. In this

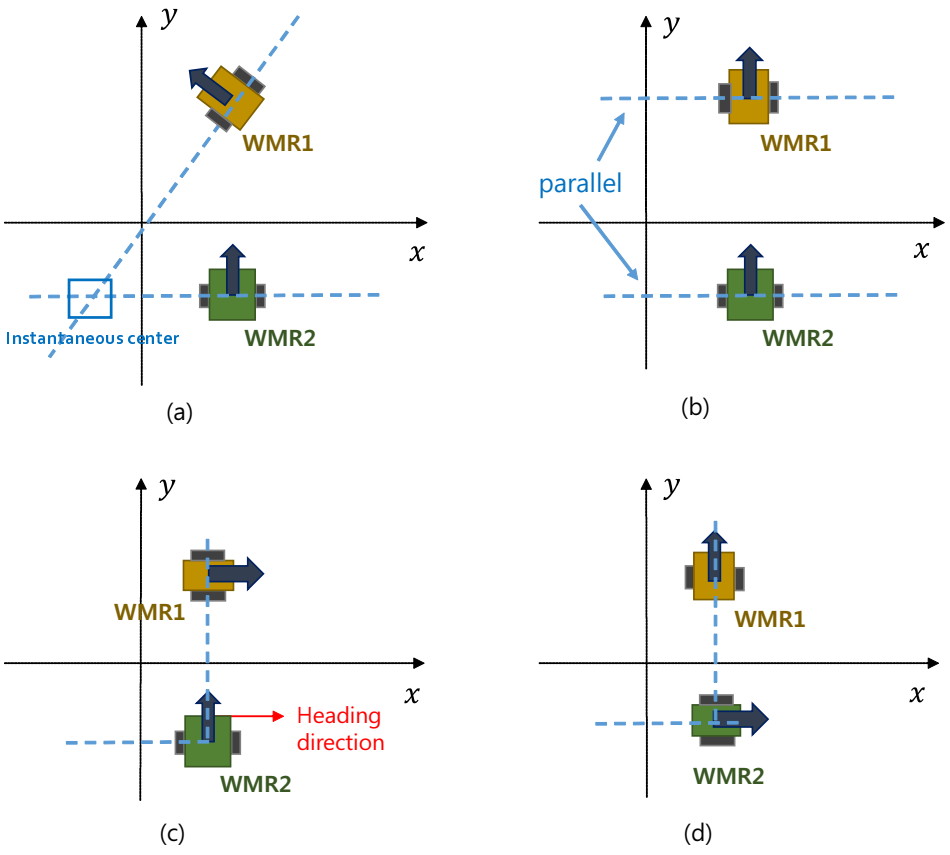

FIGURE 4.4: Variation of (ϕ_1^d, ϕ_2) for given (ω_h, v_h) and its physical representation in $\{\mathcal{I}\}$. (a): configuration for general motion about IC, (b): configuration for straight motion, (c),(d): configuration for singularity.

configuration, motion doesn't be generated physically at the moment. Note that the singularity was also described in Sec. 3.1.1 and Fig. 3.2.

Case 4. $(\omega_h = 0, v_h = 0)$:

In *case* 4, we get the result that $u = 0$ from (4.7) and, by (4.5), ϕ_1^d and ϕ_2 are

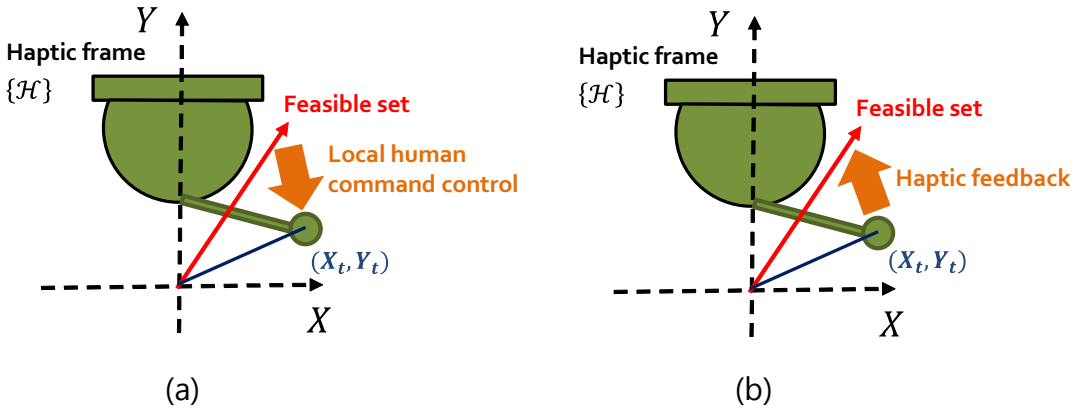

FIGURE 4.5: (a):local control to follow human command, (b):haptic feedback. (a) draws feasible set toward $(\mathrm{X}_t, \mathrm{Y}_t)$, (b) draws $(\mathrm{X}_t, \mathrm{Y}_t)$ toward feasible set. where $(\mathrm{X}_t, \mathrm{Y}_t)$ is interpretation of human command (ω_h, v_h) in $\{\mathcal{H}\}$

randomly selectable. In other words, This configuration corresponds to stop of the two WMRs because of the condition of *case* 4, i.e., $\omega_h = 0$, $v_h = 0$. Thus, this is reasonable to the result that ϕ_1^d and ϕ_2 are randomly selectable.

With the set value ϕ_1^d in (4.6), we design local low-level control $\dot{\phi}_1$ to follow human command s.t.

$$\dot{\phi}_1 = \frac{d\phi_1^d}{dt} - k_L(\phi_1 - \phi_1^d) \tag{4.8}$$

where $\dot{\phi}_1$, ϕ_1, k_L are control input, 1^{st} WMR's measured position , and control gain respectively. Note that $\frac{d\phi_1^d}{dt}$ can be obtained by numerical differentiation. The equation (4.8) is nothing but $\dot{e} + k_L e = 0$, where $e = \phi_1 - \phi_1^d$. The control $\dot{\phi}_1$ draws feasible motion toward human command.

To simply describe the local low-level control $\dot{\phi}_1$, Let's see the Fig. 4.5(a). In the figure, let us denote the interpretation of the human command (ω_h, v_h) via $\{\mathcal{H}\}$ by X_t,Y_t. Here, we set $\mathrm{X}_t = \omega_h$, $\mathrm{Y}_t = v_h$. The feasible set then is expressed by the red arrow. The thick arrow of obliquely downward direction indicates direction of local control $\dot{\phi}_1$ because the control $\dot{\phi}_1$ draws current state ϕ_1 toward human command ϕ_1^d.

4.4 Haptic Feedback

To adjust teleoperation strategy, human user needs to perceive how much his command violates feasible motion of WMRs under mixed constraint. Therefore, we utilize feasible set, which describes the feasible motion of WMRs in $\{\mathcal{H}\}$. Although other modalities are also possible, we design haptic feedback which perceives separation between the feasible set and interpretation of human command. For this, feasible set and human command interpretation should be expressed in same frame. (i.e., haptic frame $\{\mathcal{H}\}$)

With feasible set (4.4) and $(\mathrm{X}_t,\mathrm{Y}_t)$ immediately defined in Sec. 4.3, we obtain their separation in $\{\mathcal{H}\}$. Between the feasible set and interpretation of human command, i.e., human command, the separation is converted to certain force τ s.t.

$$\tau = -k_h \left(\begin{bmatrix} \mathrm{X}_t \\ \mathrm{Y}_t \end{bmatrix} - proj_{\mathrm{Y}=\frac{L\cos(\phi_1-\phi_2-\frac{\pi}{6})}{\sin(\phi_1-\phi_2)}\mathrm{X}} \begin{bmatrix} \mathrm{X}_t \\ \mathrm{Y}_t \end{bmatrix} \right) \tag{4.9}$$

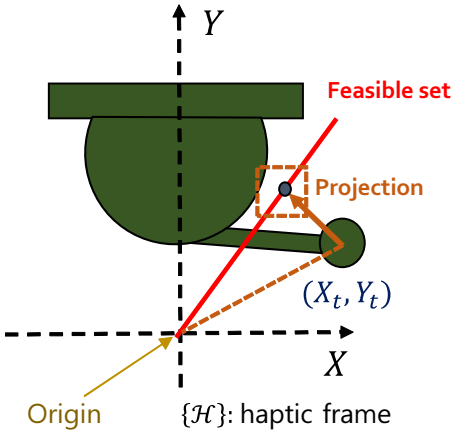

FIGURE 4.6: In constrained teleoperation, we design haptic feedback using projection of human command onto feasible set.

where k_h is haptic feedback gain and τ is haptic feedback force. Thus, the haptic feedback τ is reflection of feasible set and human command. From the haptic feedback (4.9), the feedback τ is nothing but conversion of projection of (X_t,Y_t) onto the feasible set as Fig. 4.6.

Meanwhile, in Fig 4.5(b), the thick arrow of obliquely upward direction indicates direction of the haptic feedback τ. This situation is the opposite to the Fig. 4.5(a). In Fig. 4.5(a), the local control to follow human command, i.e., human command control, draws the feasible set toward the human command. On the other hands, in Fig. 4.5(b), the haptic feedback draws the human command toward the feasible set. In other words, human command control and haptic feedback are same in

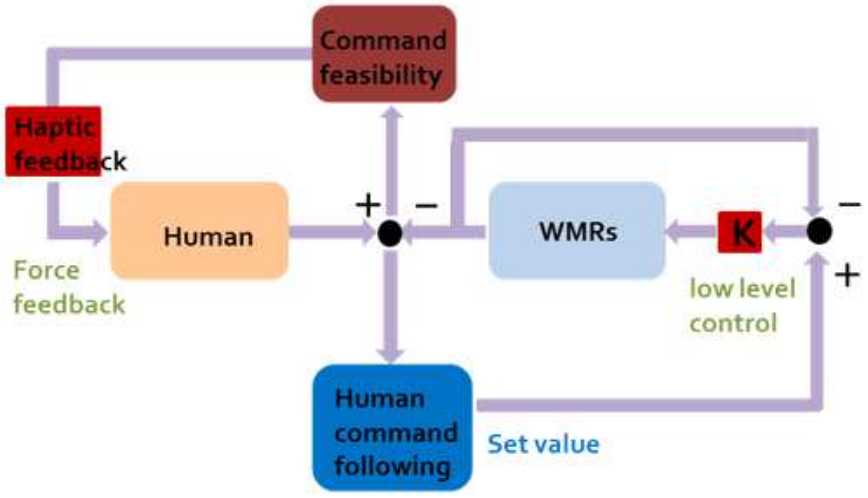

FIGURE 4.7: Interaction between human and robot including two control loops.

terms of function, but is different in that their direction. Note that, for the other application, by using concept of feasible set and human command interpretation, similar construction of haptic feedback design is also possible.

See Fig. 4.7. This figure indicates complementary interaction between human and WMRs. (i.e., master and slave) Meanwhile, we can see the two control loops in Fig. 4.7 graphically: 1) Local human command control loop includes the human command following process to find set value ϕ_1^d and the local low-level control process which sends ϕ_1 to ϕ_1^d using control $\dot{\phi}_1$ (i.e., drawing feasible set to human command); 2) Haptic feedback control loop includes the command feasibility process to find feasible set/human command interpretation and the feedback process converting into τ. (i.e., drawing human command toward feasible set). The Fig.

4.7 shows that the different two control loops run in a mutually complementary manner.

Chapter 5

Experiment

5.1 Hardware

We use our own WMR. The WMR has two wheels arranged in both sides with front and rear castor. Each wheel is driven by 24V-50Watt BLDC geared encoder motor, which has resolution of 256 CPT (counts per turn) from Maxon®. Meanwhile, for its low-level actuation, we use a servo amplifier which supports the encoder feedback in driver-level and 32-bit micro-controller with 512 KBytes programmable flash memory based on ARM Cortex-M3 from Atmel®. Its size is 220x220x130 mm, and maximum available velocity is 0.75 m/s. This nonholonomically constrained WMR's low-level control input is velocity of wheel on both sides and each wheel's velocity is easily transformable to forward and angular

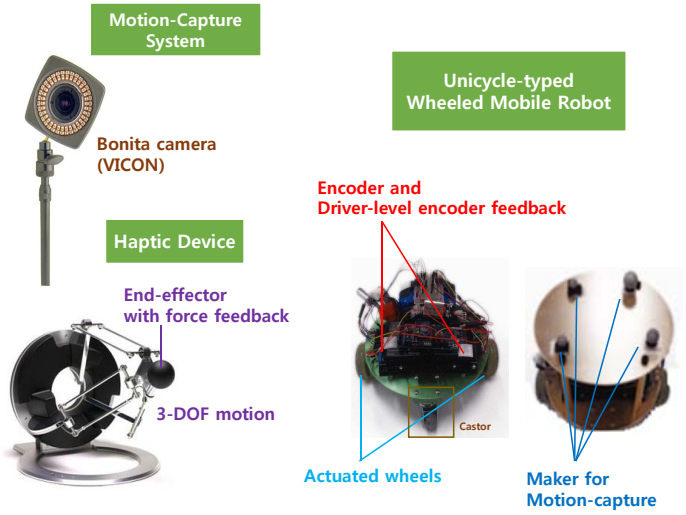

FIGURE 5.1: Individual hardware:1) motion-capture system, 2) haptic device as master, 3) unicycle-typed WMR as slave.

velocity as [29]:

$$v = \frac{r(\omega_{m,1}) + r(\omega_{m,2})}{2} \tag{5.1}$$

$$\omega = \frac{r(\omega_{m,1}) - r(\omega_{m,2})}{2l} \tag{5.2}$$

where v, ω is forward, angular velocity of the WMR, and $r, l, \omega_{m,i}$ is the radius of wheel, half length of the WMR and i-th wheel's velocity respectively. Thus, this transformed forward, angular velocity are kinematic inputs for our system.

(i.e., $\dot{q} = D_{\top}[v_1; \omega_1; v_2; \omega_2]$ in Sec. 2). Further, for its control, we use motion-capture system VICON® to measure translational, rotational data with 100 Hz. Although other measurement units can be available, (e.g., IMU sensor, camera) we use VICON® because the state estimation is not our interest in this thesis. As a master haptic device, we use Omega3 from Force Dimension®, which is 3-DOF actuated haptic device. Its resolution, translational maximum force are 0.01 mm and 12 N with stiffness 14.5 N/mm, and rate is supported by 8 KHz. For teleoperation and communication between WMRs and Omega3, we use Xbee-PRO®, which is data protocol RF module. Used the newest version of Xbee-PRO® has the ability to transmit in 250Kbps rates and it is equipped with the WMR and external computer to transmit data for each other. See. Fig. 5.1 and check the individual hardware.

5.2 Experiment Setup

To implement performance and usefulness of our proposed framework, we construct the artificial environment, whose size is 5x5 m, with several obstacles as Fig. 5.2.

A human stand up in sideway and tele-drive the WMRs from view of $\{\mathcal{B}\}$ of one WMR. In our scenario, the two WMRs cooperatively transport a common deformable object while squeezing it. For this, we install a tool with a roller bearing to squeeze/transport the grasped object. To successful tele-drive, grasping shape

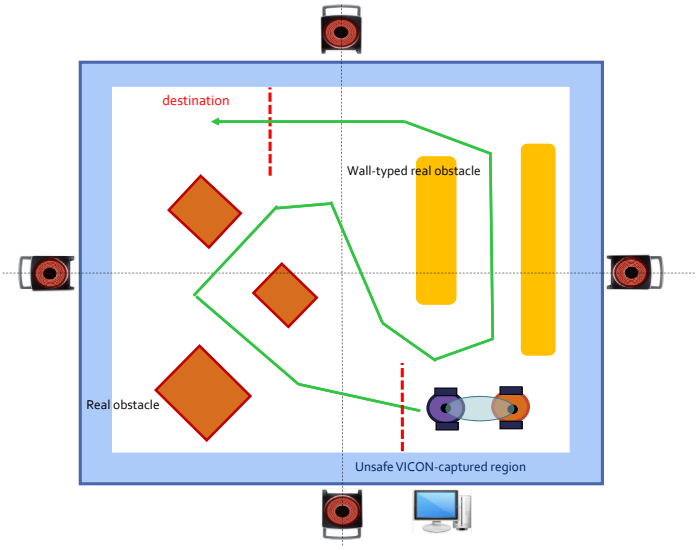

FIGURE 5.2: Graphical representation of constructed environment.

should be guaranteed by priority. Also, in the place like Fig. 5.2, because a human drives the WMRs while avoiding obstacles, aggressive steering would be necessarily involved. In our guess, the more a human drives the WMRs aggressively, the more separation between feasible set and human command may occur. As a result, our teleoperation strategy may be failed due to their separation. To deal with this separation, we include not only local human command control but also haptic feedback in our teleoperation strategy. As mentioned in Sec. 4, each of these decreases separation between feasible set and human command. Including these, we would be able to tele-drive aggressively in the place like Fig. 5.3.

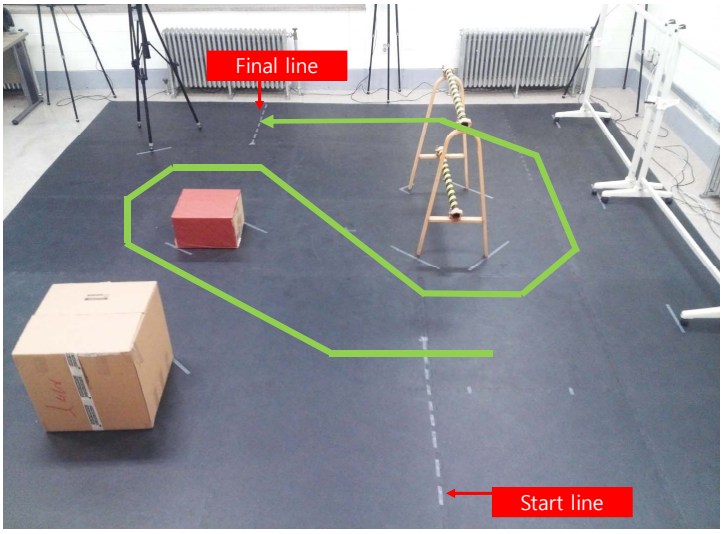

FIGURE 5.3: Real constructed environment and pre-determined route.

With setup like these, here, we perform experiment. In Sec. 5.3, we suggest detailed results and analyses.

5.3 Experiment Results

With the setup in Sec. 5.2, we perform experiments. We set the human command control gain $k_L = 5.0$, shape system gain $k_E = 0.36$, grasping shape $L = 5.3$, and haptic gain $k_h = 125$.

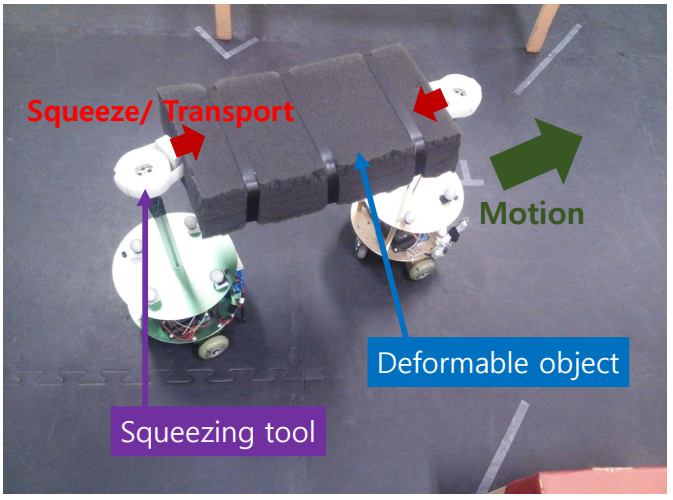

FIGURE 5.4: Real experiment: Two WMR transport a common deformable object while squeezing it.

Fig. 5.4 shows that real experiment is performed by the two WMRs transporting/squeezing a common deformable object in our constructed environment. If the grasping shape control doesn't work well or there is coupling with locked system, the pair of WMRs would drop the squeezingly grasped object. From this, observing whether the pair drop it or not, we directly can evaluate the grasping shape of the pair.

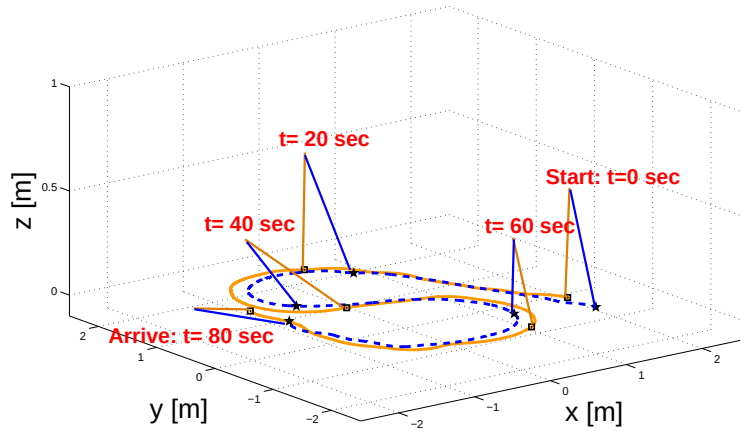

FIGURE 5.5: Trajectories of two WMRs in Real experiment

In Fig. 5.5, we can see the real trajectories of two WMRs. The human user makes an effort to tele-drive the two WMRs with the appointed route pre-determined in Fig. 5.2. The orange line is leader WMR and the blue dotted line is follower. When the user teleopearate the overall motion of two WMRs, the two WMRs autonomously grasp the common object as Fig. 5.4.

See. Fig. 5.6(a). The grasping shape error E_s is defined by difference between actual distance and L. In the figure, the WMRs arrive in destination at about 80 sec. Maximum of E_s is 0045 m, and average of that is 0.0009 m. Fig. 5.6(a) shows that grasping shape error is bounded although relatively aggressive teleoperation was performed. From this, we conclude our autonomous control for rigid-grasp control works well and can be applied to other overly constraint system.

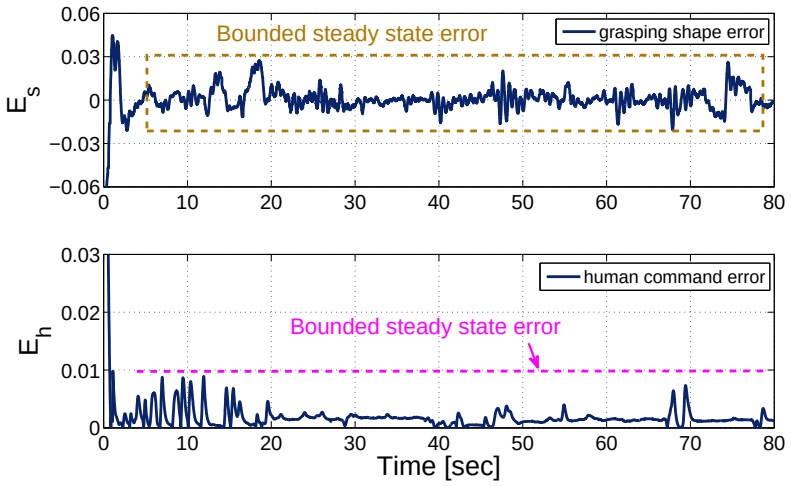

FIGURE 5.6: Grasping shape error E_s and human command error E_h have bounded steady state error.

To inspect the effect of human command control, from Fig. 5.6(b), we can see that human command error has bounded steady state error. The error E_h is defined by $\|\phi_1 - \phi_1^d\|$. Maximum of E_h is initially 0.49 rad, and average of that is 0.003 rad. Also, from initial error, E_h rapidly converges to steady state error value, which is approximatively 0.01 rad. Considering that the steady state value 0.01 rad corresponds to 0.57°, which is practically tolerable value. When $\phi_1 \to \phi_1^d$, the pair of WMRs approach to human command. Note that local human command is designed to draw the pair toward human command as much as permissible by mixed constraint. Thus, we conclude that local human command control runs properly.

We can see whether haptic feedback is operated well or not from Fig. 5.7. As

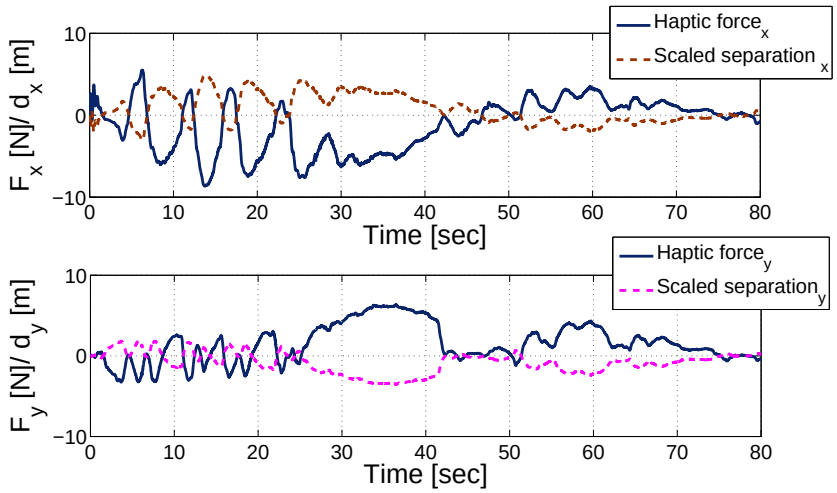

FIGURE 5.7: Haptic feedback force decreases separation between feasible set and human command. The value d=0 means that there is no separation, i.e., human command lies in feasible set.

human command control, haptic feedback decreases separation between feasible set and human command. The dark-blue line is haptic force and the other dotted line is the scaled x,y-separation. The above and bottom indicates plot of x,y-direction respectively. These graphs shows variation of haptic force and separation between feasible set and human command as time goes on. In 25-35 sec, the human command is separated from the feasible set while the haptic force is applied to opposite direction. The human command then goes to the feasible set by the haptic force. A similar aspect happens in 50-60 sec. Conceptually, haptic feedback is designed to inform the user of feasible command direction, i.e., feasible set. In experiment, this reporting is realized by haptic force. In other words, the human is informed by the haptic feedback force. Thus, the human command

move toward feasible set by the haptic force and, here, we conclude that our haptic feedback is effective and applicable to real application.

Chapter 6

Conclusion and Future Work

6.1 Conclusion

In this thesis, we present a novel framework of haptic teleoperation of a pair of WMR under overly constrained system, which enables remote human user to teleoperate overall motion while cooperatively squeeze/grasp a common deformable object. For this, utilizing NPD [1, 2], we mathematically decompose the overall motion into locked system and grasping shape system, while feasible set is derived from our haptic interface. Utilizing these items, we design local autonomous control following human command and haptic feedback. Conceptually, Haptic feedback and local human command control are designed to inform the user of feasible command direction and draw the pair toward human command

respectively. In experiment, we get the result that local shaped control, human command control, and haptic feedback work well. Throughout this thesis, not only NPD-based virtual rigid-grasp constraint control under no-slip condition but also a novel semi-autonomous control architecture for constrained teleoperation is proposed and experimental results also support the theory.

6.2 Future Work

This thesis includes the results of first-step using our proposed framework. To summarize, possible future topics includes: 1) Extension of semi-autonomous architecture to other overly constrained systems; 2) Experiments in outdoor environment using vision; 3) User study to look into the effects of proposed architecture more deeply. In other words, by extending the theory, with extended/modified mathematical expression, the proposed control architecture isn't restricted to certain overly constrained system. Further, to inspect the possibilities via real applications, experiments would be more needed without motion-capture system and, to illustrate the effect of our proposed design more generally/deeply, we need to perform the more experiments with the more people, e.g., user study.

Bibliography

[1] D.J. Lee. Passive decomposition and control of nonholonomic mechanical systems. *IEEE Transactions on Robotics*, 26(6):978–992, 2010.

[2] D.J. Lee. Passive decompostion of multiple nonholonomic mechanical systems under motion coordination requirements. In *Proc. IFAC World Congress*, 2008.

[3] P. Malysz and S. Sirouspour. Trilateral teleoperation control of kinematically redundant robotic manipulators. *The International Journal of Robotics Research*, 30(13):1643–1664, 2011.

[4] W. Dong and J.A. Farrell. Cooperative control of multiple nonholonomic mobile agents. *IEEE Transactions on Automatic Control*, 53(6):1434–1448, 2008.

[5] Jaydev.P. Desai, James.P. Ostrowski, and Vijay. Kumar. Modeling and control of formations of nonholonomic mobile robots. *IEEE Transactions on Robotics and Automation*, 17(6):905–908, 2001.

[6] P. Tabuada, G.J. Pappas, and P. Lima. Motion feasibility of multi-agent formations. *IEEE Transactions on Robotics*, 21(3):387–392, 2005.

[7] Li. Xiaohai, J. Xiao, and Z. Cai. Backstepping based multiple mobile robots formation control. In *Proc. IEEE/RSJ Int'l Conference on Intelligent Robots and Systems*, pages 887–892. IEEE/RSJ, 2005.

[8] Hiroaki. Yamaguchi and J.W. Burdick. Asymptotic stabilization of multiple nonholonomic mobile robots forming group formations. In *Proc. IEEE Int'l Conference on Robotics and Automation*, pages 3573–3580. IEEE, 1998.

[9] X. Yun and Yoshio. Yamamoto. Stability analysis of the internal dynamics of a wheeled mobile robot. *Journal of Robotic Systems*, 14(10):697–709, 1997.

[10] Z. Zuo and D.J. Lee. Haptic tele-driving of a wheeled mobile robot over the internet: a pspm approach. In *Proc. IEEE Conference on Decision and Control*, pages 3614–3619. IEEE, 2010.

[11] B.M. Kim and P. Tsiotras. Controllers for unicycle-type wheeled robots: Theorectical result and experiment validation. *IEEE Transactions on Robotics and Automation*, 18(3):294–307, 2002.

[12] O. Khatib, K. Yokoi, K. Chang, D. Ruspini, R. Holmberg, and A. Casal. Coordination and decentralized cooperation of multiple mobile manipulators. *Journal of Robotic Systems*, 13(11):755–764, 1996.

[13] Homayoun Seraji. A unified approach to motion control of mobile manipulators. *The International Journal of Robotics Research*, 17(2):107–118, 1998.

[14] H.S. Yang and D.J. Lee. Cooperative grasping control of multiple mobile manipulators with obstacle avoidance. In *Proc. IEEE Int'l Conference on Robotics and Automation*, pages 828–833. IEEE, 2013.

[15] Y. Yamamoto and Xiaoping Yun. Coorninating locomotion and manipulation of a mobile manipulator. In *Proc. IEEE Conference on Decision and Control*, pages 2643–2648. IEEE, 1992.

[16] D.J. Lee and M.W. Spong. Bilateral teleoperation of multiple cooperative robots over delayed communication networks: Theory. In *Proc. IEEE Int'l Conference on Robotics and Automation*, pages 360–365. IEEE, 2005.

[17] D.J. Lee and M.W. Spong. Bilateral teleoperation of multiple cooperative robots over delayed communication networks: Application. In *Proc. IEEE Int'l Conference on Robotics and Automation*, pages 366–371. IEEE, 2005.

[18] R.J. Anderson and M.W. Spong. Bilateral control of teleoperation with time delay. *IEEE Transactions on Automatic Control*, 34(5):494–501, 1989.

[19] D.J. Lee and Ke. Huang. Passive-set-position-modulation framework for interactive robotic systems. *IEEE Transactions on Robotics*, 26(2):354–369, 2010.

[20] G. Niemeyer and J.E Slotine. Telemanipulation with time delays. *The International Journal of Robotics Research*, 23(9):873–890, 2004.

[21] D.A. Lawrence. Stability and transparency in bilateral teleoperation. *IEEE Transactions on Robotics and Automation*, 9(5):624–637, 1993.

[22] J.R.T. Lawton, R.W. Beard, and B.J. Young. A decentralized approach to formation maneuvers. *IEEE Transactions on Robotics and Automation*, 19.

[23] D.J. Lee, A. Franchi, H.I. Son, C.S. Ha, H.H. Bülthoff, and P.R. Giordano. Semi-autonomous haptic teleoperation control architecture of multiple unmanned aerial vehicles. *IEEE/ASME Transactions on Mechatronics*, 18(4):1334–1345, 2013.

[24] C.S. Ha and D.J. Lee. Vision-based teleoperation of unmanned aerial and ground vehecles. In *Proc. IEEE Int'l Conference on Robotics and Automation*, pages 1465–1470. IEEE, 2013.

[25] A. Franchi, P.R. Giordano, C. Secchi, H.I. Son, and H.H. Bülthoff. A passivity-bassed decentralized approach for bilateral teleoperation of a group of uavs with switching topology. In *Proc. IEEE Int'l Conference on Robotics and Automation*, pages 898–905. IEEE, 2011.

[26] D.J. Lee and Ke. Huang. Peer-to-peer control architecture for multiuser haptic collaboration over undirected delayed packet-switching network. In *Proc. IEEE Int'l Conference on Robotics and Automation*, pages 1333–1338. IEEE, 2010.

[27] M.W. Spong, S. Hutchinson, and M. Vidyasagar. *Robot Modeling and Control*. WILEY, 2006.

[28] R.M. Murray, Z. Li, and S.S. Sastry. *A mathematical introduction to robotic manipulation*. CRC, 1993.

[29] R. Siegwart, I.R. Nourbakhsh, and D. Scaramuzza. *Introduction to Autonomous Mobile Robots*. MIT Press, 2011.

요 약

본 논문에서는 극도로 제한된 시스템하에서의 한 쌍의 이동로봇의 원격조종 기법에 대해서 기술한다. 논문에서 제시한 제어기법을 통해 사용자가 원격제어로 전체 이동로봇 팀을 조종할 수 있으며, 동시에 공통의 변형가능한 물체를 협력적으로 움켜쥐며 수송할 수 있다. 이를 위해 Nonholonomic passive decomposition [1, 2] 을 기초로 하여 전체 이동로봇의 움직임을 두 가지 측면으로 나누었으며, 이 과정에서 이동로봇의 실현가능한 움직임의 집합들을 정의하였다. 또한 이를 이용하여 사용자명령을 따라가는 원격조종제어와 햅틱 피드백제어를 디자인하였고, 위에서 나누어진 모양을 맞추는 움직임에 대한 측면을 따로 자동제어하여 이동로봇이 변형가능한 물체를 자동으로 움켜쥐면서 협력적으로 수송할 수 있게 하였다. 더불어 제안된 제어기법에서는 사용자명령을 따라가는 원격조종제어와 햅틱 피드백제어가 극도로 제한된 시스템 하에서의 이동로봇팀이 자연스럽게 움직일 수 있도록 원격 조종을 도와줄 수 있음을 보인다. 마지막으로 실험결과를 제시한다.

주요어: Asymmetric teleoperation, Mixed constraint, Wheeled mobile robot, Haptic feedback, Semi-autonomous, Feasibility

학번: *2012-23193*